Research Square

Preprints are preliminary reports that have not undergone peer review. They should not be considered conclusive, used to inform clinical practice, or referenced by the media as validated information.

Spectral Matching of Three-Component Seismic Ground Accelerations for Nuclear Power Plants

Sindur Mangkoesoebroto (sindurpm@gmail.com)
Institute of Technology Bandung: Institut Teknologi Bandung https://orcid.org/0000-0003-2888-0532

Ediansjah Zulkifli
Institute of Technology Bandung: Institut Teknologi Bandung

Adi P. Yasa
Institute of Technology Bandung: Institut Teknologi Bandung

Research Article

Keywords: Spectral matching, three components, components couplings, phase angle, baseline correction

Posted Date: June 16th, 2021

DOI: https://doi.org/10.21203/rs.3.rs-613198/v1

License: This work is licensed under a Creative Commons Attribution 4.0 International License.
Read Full License

Spectral Matching of Three-Component Seismic Ground Accelerations for Nuclear Power Plants

Sindur P. Mangkoesoebroto[1*], Ediansjah Zulkifli[1], Adi P. Yasa[2]

[1]*Civil Engineering Department, Institute of Technology Bandung, Jalan Ganesha 10, Bandung 40132, Indonesia*

[2]*Center for Industrial Research, Institute of Technology Bandung, Jalan Ganesha 10, Bandung 40132, Indonesia*

** Corresponding author sindurpm@gmail.com*

Abstract. The aim of the paper is to introduce a new procedure of three-component spectral matching of seismic ground acceleration records. The procedure is straightforward, yet it is general. In principle, the procedure involves varying of both the Fourier amplitude and the phase spectra so that the modified records' spectra agree with a target. The matching can be performed against either a target Fourier or response spectra. In the former the solution is exact, while in the latter it becomes approximate. A target spectrum representative of three directions should be provided. In the example several three-component records were matched against two target spectra. Good convergence was achieved in velocity and displacement records so that no baseline correction was necessary. The couplings among the components were preserved.

Keywords: Spectral matching, three components, components couplings, phase angle, baseline correction

1. Introduction

In seismic design of structures, systems, and components (SSCs) of nuclear power plants (NPPs) the need of realistic ground motions is the most critical issue. It is highly recommended using actual (three-component) earthquake motions whose spectra are close to the specified ones to produce a realistic response of the SSCs (ASCE/SEI, 2005).

However, the ground motion records of such earthquakes for a particular site are rarely available (Wang et. al., 2014). In this case an ensemble of derived records needs to be generated via synthetic procedure or spectral matching of actual records. Key parameters to be observed are the couplings among the three components, the Fourier amplitudes and phases, and the durations. This study is aimed at proposing a consistent procedure to generate spectrum compatible three-component seismic ground accelerations based on actual records.

For one-component spectral matching, the procedure has been a subject of intense discussions for many years as inappropriate techniques have showed bias in the estimated structural response (e.g., Luco and Bazzurro, 2007). In this scenario, the modified record is obtainable by several ways, but all can be summarized into one mathematical operation following this expression,

$$|A_m(\omega,t)|\, e^{i\phi_{A_m}(\omega,t)} = |P(\omega,t)|\,|A_s(\omega,t)|\, e^{i\left[\phi_P(\omega,t)+\phi_{A_s}(\omega,t)\right]} \quad . \tag{1}$$

In the expression, $A_s(\omega,t) = |A_s(\omega,t)|\, e^{i\phi_{A_s}(\omega,t)}$ is the nonstationary seed or initial acceleration to be adjusted, which can be actual or synthetic records uniquely characterized by their amplitudes and phases; and $P(\omega,t)$ is a generalized filter function. When a synthetic record is desired, the initial stationary record is generated based on a specified function of a power spectrum by assuming the phase is uniformly distributed over [-π,π]. The record is then multiplied by a nonstationary envelope function and is transformed to frequency domain for further processing in accordance with the above expression so that the spectrum of the adjusted acceleration is compatible with a selected target spectrum (e.g., Preumont, 1984; Thrainsson et. al., 2000; Bani-Hani and Malkawi, 2017).

The adjustment is carried out by filtering the initial record by a filter function whose magnitude and phase are so chosen that the adjusted record satisfies the desired

properties. The filter function, $P(\omega,t)$, can be viewed as a two-dimensional spectral ratio filter function in its most generality, with one axis as its amplitude, $|P(\omega,t)|$, and the other is its phase, $\phi_P(\omega,t)$. The filtering process can be performed by varying the amplitude alone, the phase, or both. The simplest one, commonly known as spectral scaling, is by fixing the amplitude at a specified constant value and setting the phase of the filter function to be identically zero. This will result in the modified record having the identical phase to the seed, and its Fourier amplitude being proportional to the original record. When transformed back to the time domain, the adjusted record is proportional in its acceleration values with respect to the original one without changed in its duration. This change in the acceleration but none in the duration clearly will change its time derivatives, or the jerk, which is the first derivative of the acceleration (He et. al., 2015). Studies on a SDOF structure subjected to such scaled records have been conducted (e.g., Carballo and Cornell, 2000; Luco and Bazzurro, 2007; Bazzurro and Luco, 2006). Their conclusion, among others, was, while there was negligible bias in the linear systems, the biases were observed in the nonlinear ones. In the up-scaled record, depending on the scaling factor, the bias was higher compared to the un-scaled one.

In other scenario, known as the spectral matching, the record modification was conducted by varying the amplitude of the filter function in limited range while letting its phase to be randomly distributed. When transformed back to time domain, this technique would produce records with little change in duration. In fact, this technique was performed in time domain by adjusting an actual acceleration record either by adding wavelets to the record (Kaul, 1978; Lilhanand and Tseng, 1988; Abrahamson, 1992; Mukherjee and Gupta, 2002; Suarez and Montejo, 2005; Hancock et. al., 2006; Al Atik and Abrahamson, 2010; Gao et. al., 2014; Adekristi and Eatherton, 2016; Hong and Huang,

2020; Roman-Velez and Montejo, 2020), or by decomposing the original record into mode functions, adjust them and then recombined the functions (e.g., Ni et. al., 2011; Li et. al., 2016), or using some stochastic methods (e.g., Pousse et. al., 2006; Laurendeau et. al., 2012; Zentner, 2013; Waezi and Rofooei, 2017), or artificial neural network (e.g., Ghaboussi and Lin, 1998; Lee and Han, 2002; Ghaffarzadeh and Izadi, 2008). The aim was to modify the actual records to produce time series whose response spectra were close to the target while controlling the duration.

The time-domain spectral matching based on superposition of wavelets (Al Atik and Abrahamson, 2010) had been widely reviewed. While there were no or negligible biases in the linear response, studies showed that the nonlinear response of the resulting modified records tend to be unconservative (Seifried and Baker, 2016) compared to the actual ones; while others found they could be more aggressive or more benign than the real records (Lancieri et. al., 2018). In this scenario, the phases were, in general, assumed to be randomly distributed, though in fact, they may be not. Studies investigating the effects of the phase of the input motion had been carried out, among others, by Ohsaki (1979), Tiliouine et. al. (2000), Thrainsson et. al. (2000).

As implied by its name, the frequency domain is a technique which processed the spectral matching in the frequency domain. In this scenario the records' phase were controlled either by preserving the original phase or by replacing it with the phases from other seismic records. We believe that the phases of seismic records are not entirely random but form certain periodic patterns (see Section 3), and preserving the phases are important (Fahjan and Ozdemir, 2008) as also implied in ASCE/SEI (2005). In this scenario the filter phase should be set to zero or constant, with its amplitude to be adjusted to produce the modified records whose response spectra agree with the target.

When transformed to time domain, they produce records with change in the durations (Lilhanand and Tseng, 1987). In the past, this scenario was known to introduce drift in the displacement records, but the work by Shahbazian and Pezeshk (2010) resolved this issue. Contributors in this field were, among others, Rizzo et. al. (1975), Gasparini and Vanmarcke (1976), Kost et. al. (1978), Thrainsson et. al. (2000). Another technique combining both the time- and frequency-domain was also explored to control both the duration and the phase, while achieving agreement in the response spectra to a target spectrum (Silva and Lee, 1987).

Comparisons among the techniques, in general, showed that while biases were negligible in linear response, they could be significant in the nonlinear ones (e.g., Bazzurro and Luco 2006; Carlson et. al., 2016; Lancieri et. al., 2018). In some cases, major changes were noticed (Naeim and Lew, 1995), and in others the effect could vary from minor to significant (Zekkos et. al., 2012; Gascot and Montejo, 2016). In general, the performance of the modified record depends on (a) the mismatch of the seed and the target spectra, (b) the characteristic of the seed records (e.g., pulse or non-pulse types), and (c) the spectral matching techniques such as described above (e.g., Shahbazian and Pezeshk, 2010; Carlson et. al., 2016). The matching process should preserve as many key parameters as possible as they might play important role. In addition to spectral amplitude, the parameters such as the duration, the jerk and the phase need to be controlled (Fahjan and Ozdemir, 2008). Replacing the phase record with that of others can yield modified records of the same peak ground acceleration but entirely different nonlinear SDOF response (Tao et. al., 2019).

The procedures were commonly applied to match one component of the seismic ground accelerations. In the past, researchers (e.g., Preumont, 1984; Li et. al., 2016)

proposed the matching be carried out for one component separately and then combined them to form the three-component ground accelerations. This procedure created problems as how to synchronize their peak amplitudes as the coupling among the components might have effects on the structural response. Herein, the problem will be resolved by introducing a single filter function that operates on a vector of three components.

The use of a single filter function to match all three components simultaneously requires a single target spectrum representative of three orthogonal directions. Although this is not the scope of the present study, however, the target spectrum, in principle, can be constructed as a geometric mean or a SRSS (square root of the sum of the squares) combination of the horizontal and the vertical spectra. The vertical smooth spectra can be obtained based on the horizontal spectra by modifying its period and amplitude, normally regulated in seismic codes (e.g., ASCE/SEI, 2005), or, by employing the relations available for the ratio of the vertical-to-horizontal spectra (e.g., Bozorgnia and Campbell, 2016), from which a single target spectrum can be created. The spectrum should be used as a reference in selecting the seed records whose spectral mismatch is minimal (e.g., Wang et. al., 2014; Kohrangi et. al., 2017; Baker and Lee, 2018). An average spectrum developed based on a consistent approach (see Section 3), of all seed records should be produced and compared to the target to ensure that reasonably small mismatch is observed.

The development is started with a linear simple oscillator excited in three perpendicular directions by stochastic ground acceleration. The motion in each direction is associated with each component, and its dynamical properties, spring, and damping, is identical in all directions or isotropic, and are constants. The problem formulation is discussed next.

2. Problem Formulation

The nonstationary equation of motion of a linear simple oscillator with three orthogonal degree of freedom systems is (e.g., Papadimitriou, 1990; Bougioukou et. al., 2008),

$$\mathbf{M}\frac{d^2}{dt^2}\mathbf{u}(t,\tau)+\mathbf{C}\frac{d}{dt}\mathbf{u}(t,\tau)+\mathbf{K}\,\mathbf{u}(t,\tau)=-\mathbf{M}\,\mathbf{a}(t,\tau) \tag{2}$$

where **M**, **C**, and **K** are 3 x 3 mass, damping, and stiffness matrices, respectively, assumed to be constants; $\mathbf{u}(t,\tau)$is the three-component displacement vectors of the oscillator, and $\mathbf{a}(t,\tau)$ is the three-component translational ground acceleration vector. In Eq. (2) $\mathbf{u}(t,\tau)$is the nonstationary displacement vector defined as $\mathbf{u}(t,\tau)=\mathbf{u}(t)\,w(t-\tau)$ in which $\mathbf{u}(t)$ is the stationary displacement variable and $w(t)$ is a density function; t, τ are both time variables. It is obvious that the stationary displacement variable can be obtained by integrating its nonstationary counterpart over τ. The concept is applicable to other time or frequency dependent variables as well.

For isotropic system analysed in its three orthogonal principal directions excited by seed ground acceleration, Eq. (2) becomes,

$$\frac{d^2}{dt^2}\mathbf{u}_s(t,\tau)+2\zeta\omega_n\frac{d}{dt}\mathbf{u}_s(t,\tau)+\omega_n{}^2\,\mathbf{u}_s(t,\tau)=-\mathbf{a}_s(t,\tau) \tag{3}$$

where $\mathbf{a}_s(t,\tau)=(a_{s1}(t,\tau),a_{s2}(t,\tau),a_{s3}(t,\tau))$, similarly for $\mathbf{u}_s(t,\tau)$, ζ is the damping, and ω_n is the system's natural frequency; ζ, ω_n are constants. The solution of Eq. (3) for the displacement in the frequency domain is,

$$\mathbf{U}_s(\omega,t)=-H(\omega;\omega_n,\zeta)\,\mathbf{A}_s(\omega,t) \tag{4}$$

where $\mathbf{U}_s(\omega,t) \cancel{\&} \int_{-\infty}^{\infty} \mathbf{u}_s(\tau,t) e^{-i\omega\tau} d\tau = \int_{-\infty}^{\infty} \mathbf{u}_s(\tau) w(\tau - t) e^{-i\omega\tau} d\tau$ is the nonstationary Fourier transform of $\mathbf{u}(t,\tau)$, $H(\omega;\omega_n,\zeta) = |H(\omega;\omega_n,\zeta)| e^{i\phi_H(\omega;\omega_n,\zeta)}$ is the frequency response function, with $|H(\omega;\omega_n,\zeta)| = \frac{1}{\omega_n^2} \sqrt{\frac{1}{\left[1-(\omega/\omega_n)^2\right]^2 + \left[2\zeta\omega/\omega_n\right]^2}}$, $\tan\phi_H(\omega;\omega_n,\zeta) = \frac{2\zeta\omega/\omega_n}{1-(\omega/\omega_n)^2}$, and $\mathbf{A}_s(\omega,t) \cancel{\&} \int_{-\infty}^{\infty} \mathbf{a}_s(\tau,t) e^{-i\omega\tau} d\tau = \int_{-\infty}^{\infty} \mathbf{a}_s(\tau) w(\tau - t) e^{-i\omega\tau} d\tau$ is the nonstationary Fourier transform of the seed ground acceleration vector. It should be emphasized that the right side of Eq. (4) contains two kinds of phases; the first one being the phase between the motion and the response embedded in the response function, and the second one is the Fourier phase built-in in the ground acceleration.

The nonstationary Fourier amplitude spectrum (*FAS*) of $\langle \mathbf{U}_s \rangle = \mathbf{U}_s(\omega,t)$ defined as $FAS_{\langle \mathbf{u}_s \rangle}{}^2 = \langle \mathbf{U}_s \rangle \bullet \langle \mathbf{U}_s \rangle^*$, where the symbol $\bullet$ is for the inner product and * for the conjugate, is obtained as,

$$FAS_{\langle \mathbf{u}_s \rangle}(\omega,t) = |H(\omega;\omega_n,\zeta)| \; FAS_{\langle \mathbf{a}_s \rangle}(\omega,t) \tag{5}$$

From which it can be deduced that the nonstationary property of the response in time axis is the same as that of the ground acceleration; but in frequency axis it is modified by the response function. Now suppose that the ground motion is modified into $\langle \mathbf{a}_m \rangle$ then the nonstationary Fourier amplitude spectrum of $\mathbf{U}_m(\omega,t)$ is similarly obtainable as,

$$FAS_{\langle \mathbf{u}_m \rangle}(\omega,t) = |H(\omega;\omega_n,\zeta)| \; FAS_{\langle \mathbf{a}_m \rangle}(\omega,t) \tag{6}$$

Let a function $P(\omega,t)$ be the ratio of Eq. (6) with respect to Eq. (5), then the following two equations hold,

$$FAS_{\langle \mathbf{u}_m \rangle}(\omega,t) = |P(\omega,t)| \, FAS_{\langle \mathbf{u}_s \rangle}(\omega,t) \tag{7}$$

$$FAS_{\langle \mathbf{a}_m \rangle}(\omega,t) = |P(\omega,t)|\, FAS_{\langle \mathbf{a}_s \rangle}(\omega,t) \tag{8}$$

Eq. (8) shows that the property of $P(\omega,t) = |P(\omega,t)|\, e^{i\phi_P(\omega,t)}$, where $\phi_P(\omega,t)$ is the filter's phase or the phase difference between the matched and seed records, completely controls the modification of the seed acceleration into the modified one; while Eq. (7) indicates that adjustments of the responses are completely described by the same function. Further operation of Eq. (8) leads to the following expression, which is the basis of spectral matching,

$$\mathbf{A}_m(\omega,t) = P(\omega,t)\,\mathbf{A}_s(\omega,t) \tag{9}$$

where the indices *m* and *s* are for the modified and the seed ground accelerations, respectively, and $P(\omega,t)$ is the nonstationary Fourier spectral ratio of the modified to the seed response determined by Eq. (7). Since $\mathbf{U}(-\omega,\tau) = [\mathbf{U}(\omega,\tau)]^*$ for real $\mathbf{u}(t,\tau)$ (e.g., Press et. al., 2007) then it follows that $P(-\omega,\tau) = [P(\omega,\tau)]^*$ or $\phi_P(-\omega,\tau) = -\phi_P(\omega,\tau)$.

Eq. (9) shows that $P(\omega,t)$ preserves the coupling, or the direction cosines, among the components of the ground motion vector; and further, if it has zero-phase then it preserves the phase of the records. It is the intent of the modification that the modified record will have its spectra agrees with a target. If $P(\omega,t)$ is obtained as the Fourier spectral ratio as indicated by Eq. (7), then Eq. (9) is exact; however, when $P(\omega,t)$ is determined by the response spectral ratio (instead of the Fourier), then Eq. (9) is merely approximate. In the stationary case there is close relation between the Fourier and the velocity spectra, as follows (for low damping, $\zeta \leq 0.10$),

$$FAS_{\mathbf{u}}(\omega) \sim \sqrt{\sum_{i=1}^{3}\left\{\left(\int_0^{t_D} \mathrm{a}_i(\tau)\sin\omega\tau\, d\tau\right)^2 + \left(\int_0^{t_D} \mathrm{a}_i(\tau)\cos\omega\tau\, d\tau\right)^2\right\}} \tag{10}$$

$$S_{\mathbf{v}}(\omega) \le \max_{t} \sqrt{\sum_{i=1}^{3} \left\{ \left(\int_0^t \mathrm{a}_i(\tau) \sin \omega\tau \, d\tau \right)^2 + \left(\int_0^t \mathrm{a}_i(\tau) \cos \omega\tau \, d\tau \right)^2 \right\}} \tag{11}$$

where $FAS_{\mathbf{u}}(\omega)$, $S_{\mathbf{v}}(\omega)$ are the stationary Fourier amplitude and the velocity spectra of the displacement and velocity vectors, respectively; and t_D is the duration of the record. When we use Eq. (10) for the spectral ratio to get $P(\omega,t)$ in Eq. (9) then the modified ground acceleration is obtainable in a straightforward manner; but, when Eq. (11) is employed to compute $P(\omega,t)$ then Eq. (9) is just approximate, and iteration is necessary to solve the matching process.

The Fourier integral of Eq. (9) is the following,

$$\mathbf{a}_m(t,\tau) = \frac{1}{2\pi} \int_{-\infty}^{\infty} \mathbf{A}_s(\omega,\tau) P(\omega,\tau) e^{i\omega t} \, d\omega = \frac{1}{2\pi} \int_{-\infty}^{\infty} \int_{-\infty}^{\infty} \mathbf{a}_s(s,\tau) e^{-i\omega s} \, ds \, P(\omega,\tau) e^{i\omega t} \, d\omega \tag{12}$$

Interchange the order of integration and recognizing that $p(t,\tau) = \frac{1}{2\pi} \int_{-\infty}^{\infty} P(\omega,\tau) e^{i\omega t} \, d\omega$, one can get the following convolution integral,

$$\mathbf{a}_m(t,\tau) = \int_{-\infty}^{\infty} \mathbf{a}_s(s,\tau) \, p(\mathrm{t}-s,\tau) \, \mathrm{d}s \tag{13}$$

where $p(t,\tau)$ is real since $P(-\omega,\tau) = [P(\omega,\tau)]^*$. Eq. (13) is valid for nonstationary processes; however, when the filter function is computed based on Eq. (10) or (11) then the filter function becomes stationary and Eq. (13) can be integrated over τ to obtain its stationary counterpart as follows,

$$\mathbf{a}_m(t) = \int_0^{\mathrm{t}} \mathbf{a}_s(s) \, p(\mathrm{t}-s) \, \mathrm{d}s \tag{14}$$

where the limit of integration has been adjusted in accordance with the acceleration time series. A spectral matching based on Eq. (14) preserves the direction cosines of the

ground accelerations, but, in general, it will not preserve the records' phase, unless the filter's phase is set to zero or constant. For zero-phase filter then $P(\omega)=|P(\omega)|$ is real and even, and $p(t)$ is also real and even. If further, $P(\omega)$ is real and constant then $p(t)$ becomes the Dirac delta times the constant, and Eq. (14) can be integrated exactly to give a modified record that is proportional to the seed one, and therefore no change in the duration. Similarly, if $p(t)$ is computed based on Eq. (10) or Eq. (11) then Eq. (14) is exact or approximate, respectively. For computation, Eq. (14) is discretized as follows,

$$\mathbf{a}_m(\mathrm{t_j})=\sum_{\mathrm{k=1}}^{\mathrm{j-1}}\int_{\mathrm{t_k}}^{\mathrm{t_{k+1}}}\mathbf{a}_s(\tau)\,\mathrm{p}(\mathrm{t_j}-\tau)\,\mathrm{d}\tau \tag{15}$$

where $1\le k\le j\text{-}1, 2\le j\le n$, and n is the number of the data points. Substituting $t_{k+1}=t_k+\Delta t$, $\tau=t_k+\Delta t\,\eta$ for $0\le\eta\le 1$, $t_k=\Delta t\,k$, Eq. (15) can be written as,

$$\mathbf{a}_m(\mathrm{j})=\sum_{\mathrm{k=1}}^{\mathrm{j-1}}\int_{0}^{1}\mathbf{a}_s(\mathrm{k}+\eta)\,\mathrm{p}(\mathrm{j}+1-\mathrm{k}-\eta)\,\mathrm{d}\eta \tag{16}$$

If $\mathbf{a}_s(k+\eta)$ is a linear function of η for a piecewise linear acceleration, and similarly for the discreet filter function $p(j+1-k-\eta)$, they are expressible as,

$$\mathbf{a}_s(k+\eta)=[\mathbf{a}_s(k+1)-\mathbf{a}_s(k)]\,\eta+\mathbf{a}_s(k) \tag{17}$$

$$p(j+1-k-\eta)=\{[p(j-k)-p(j-k+1)]\;\eta+p(j-k+1)\}\{\delta(\eta)+\delta(\eta-1)\} \tag{18}$$

where δ is the Dirac delta function.

Substituting Eqs. (17) and (18) into Eq. (16) then carry out the integration and rearrange to obtain the expression for the matched ground acceleration as follows,

$$\mathbf{a}_m(j)=\sum_{k=1}^{j-1}\left[\mathbf{a}_s(k)\,p(j-k+1)+\mathbf{a}_s(k+1)\,p(j-k)\right] \tag{19}$$

where $1\le k\le j\text{-}1, 2\le j\le n$, n is the number of the data points, and $\mathbf{a}_m(1)=0$.

Eq. (19) is a straightforward, yet general, time-domain operation. Its features include: (1) the expression was derived to modify three-component ground acceleration, preserving the couplings among the components. However, when desired, it can be employed to perform one or two components record as well. (2) It can be used to modify with records' phase changed or preserved or with a prescribed phase difference (see the Appendix for further discussions). (3) It can be utilized to modify seed records based on the Fourier amplitude spectra (Tao et. al., 2019); or, more commonly adopted, based on the response spectra. When the former is the interest then the solution is exact; but if the latter is desired then iteration need to be conducted. A specified spectra representative of three directions should be provided. When one component modification is performed then $p(t)$ is associated with the spectral ratio of that component; similarly, for two components. (4) Normally, there is no need of baseline correction provided there are enough zeros in front and at the tail sides of the seed record (it can be accomplished by zero-padding). This is so because the modification may cause changes in duration, in which case there should be ample space for this duration change. If, however, there is a need for baseline correction then a simple time-domain baseline correction can be done; or, when the record's phase is to be preserved then the frequency-domain procedure can be readily implemented (Shahbazian and Pezeshk, 2010).

3. Example of Spectral Matching Based on the New Procedure

As an example, the procedure will be applied to match five seed records against a target spectrum. The records modifications in accordance with Eq. (19) is basically carried out by varying the amplitude, $|P(\omega)|$, and the phase, $\phi_P(\omega)$, of the spectral ratio filter function, $P(\omega)$, with the objective that the modified records' spectra agree with a specified one. However, in the example, we decided to preserve the records' phase, since it was

found that all records considered in the example (Table 1) exhibited certain periodic pattern in their phase spectrum (Figure 1 (left)) for three components, and at all frequency range up to 15 Hz. Though the patterns were similar for one record to the other, they could be different in the pitch and the slope of the arrow lines in Figure 1. Sometimes, there were found some dislocations of the points being unaligned with the arrow lines. The pattern supports the recommendation that the Fourier phase should be preserved (ASCE/SEI, 2005), and was reported for the first time in this article.

Firstly, a smooth spectrum as a target was devised based on ASCE/SEI (2005) provision. Subsequently, five records whose spectra were sufficiently close to the target were selected from PEER (2020) employing its provided built-in feature. Realistic results do depend on the closeness of the two (Carlson et. al., 2016), though the procedure will remain converges even when the seed spectrum is not so close to the target. Their peak ground accelerations are in the range of 0.19-0.33g.

For each record, the displacement history was then computed by using Eq. (3) for vector $\mathbf{u}_s(t)$ (after integrating both sides with respect to τ). The displacement spectrum was then determined as $S_{\mathbf{d}}(\omega,\zeta)=\max\sqrt{u_{s1}{}^2(t)+u_{s2}{}^2(t)+u_{s3}{}^2(t)}$, for ζ=5%. The pseudo acceleration and velocity spectra were defined as $S_{p\mathbf{a}}(\omega)=\omega\, S_{p\mathbf{v}}(\omega)=\omega^2\, S_{\mathbf{d}}(\omega)$. Observe that the spectra represent three-component motions in consistent manner (they were different from the target spectra which were generated by SRSS combination of the horizontal and vertical spectra). All five spectra from the seeds were then averaged to form a second target referred to as the jagged spectra. The seed records are listed in Table 1 and the spectra are presented in Figure 2. For the smooth spectra, the target peak ground acceleration and displacement are 0.3g and 14.3 cm, respectively; while that of the jagged are 0.24g and 14.3 cm.

The spectral matching of the Chuetsu-oki record, Japan, 2007, station Matsushiro Tokamachi (record ID 4843, the second in Table 1) – the station is in the vicinity area of the Kashiwazaki-Kariwa NPP – against the jagged spectra will be detailed. The accuracy of the matching procedure is measured based on the RMS error expressed as follows (Suarez and Montejo, 2005; Hancock et. al., 2006),

$$\text{Error, } e = \sqrt{\frac{1}{n_e}\sum_{k=1}^{n_e}\left[1-\frac{1}{P(k)}\right]^2} \tag{20}$$

where n_e is the number of data points within the frequency of interest (0.1-25Hz).

The procedure was conducted following these steps. (1) Compute the response spectral ratio of the target with respect to the seed, P(T) $= S_{pvt}(T) / S_{pvs}(T)$, where $S_{pvt}(T), S_{pvs}(T)$ are the pseudo velocity spectra of the target and the seed records for 5% damping, respectively; (2) Perform the inverse fast Fourier transformation of P(T) to obtain p(t); (3) Use Eq. (19) to obtain the modified ground accelerations; (4) Apply a (time domain) band-pass filter function with cut-off frequency at 0.1-25 Hz to the modified record to remove noises; (5) Compute the RMS error by Eq. (20) and calculate the average of 1/P(T) over the frequency of interest; (6) Repeat the procedure when the error and the average need to be refined. The error as computed by Eq. (20) after 14 iterations was 3.5%. The reciprocal spectral ratio (1/$P(T)$) is presented in Figure 3, and most of them are in the range of 0.90-1.10 and some in the range of 0.85-1.15 for the period range of 0.04-10.00 seconds. The average of 1/P(T) over the period of interest (0.04-10 seconds) is 1.007. These show satisfactory matching process according to ASCE/SEI (2005). Its spectra before and after the spectral matching against the jagged target are shown in Figure 4. At low periods the peak ground acceleration converged to the spectral

acceleration of around 0.24g, and at high periods the peak ground displacement approached the spectral displacement of about 14.3 cm in this example.

The major component of the jerk, acceleration, velocity, and the displacement of the seed and the matched records are shown in Figure 5. The drifts were not observable in the velocity and the displacement time series. The phase angles of each component and the couplings, or the direction cosines, among the three-component were conserved. As observed, the jerk of the seed and that of the matched records look similar without significant change in durations. The peak ground acceleration and the displacement of the matched record converged to $S_{pat}(T\rightarrow 0)$=0.24g and $S_{dt}(T\rightarrow\infty)$=14.3 cm, respectively. The acceleration Fourier amplitude spectra ($FAS_{\mathbf{a}}$) of the seed and the matched records are presented in Figure 6. It shows a marked difference between the seed and the matched records despite relatively close in their pseudo velocity spectra as shown in Figure 4. In Table 2, together with the PGA and PGD, the values of the peak ground velocity (PGV), the significant duration ($D_{05\text{-}95}$), and the Arias intensity (I_A) before and after modifications are presented. They are all higher after modifications. The phase of the matched record is indicated in Figure 1 (right) for component 2. The pattern was preserved.

The resulting spectra of all five records are shown in Figure 7, on the left for the jagged and on the right for the smooth spectra. It is observable that in general the convergence is very good; however, in the period range of 10-20 seconds, the convergence is better for the jagged than for the smooth target spectra, as the jagged spectrum is more natural as it is the result of an averaging process of real spectra in consistent manner. Nevertheless, the convergence in the period range 0.04-10 seconds is satisfactory.

Some ground motion parameters are shown in Table 3 for the peak acceleration, velocity, displacement as well as the Arias intensity and the significant duration, $D_{05\text{-}95}$.

They are presented for the target both jagged and smooth, the seed, and the matched records. For illustration, the peak ground acceleration of the target smooth spectra is 0.30g and the average of five seeds is 0.24g with its variability of 0.21. This indicated that performing the modifications gave the corresponding values of 0.28g for the average peak ground acceleration of the matched records with the variability 0.05 against the smooth target spectra. However, the variability of the jagged target spectra is lower of 0.02, and these lower numbers are consistent for all parameters (see Table 3), indicating better convergence for the jagged spectral matching. Among the five parameters shown in Table 3, low variability is observed for the peak acceleration and displacement but higher for the peak velocity, the Arias intensity and the significant duration, $D_{05\text{-}95}$. The last one is the most random considering the variability of the seed of 0.18 and those of the matched records of 0.20 and 0.14 for the smooth and the jagged spectra, respectively; based on the limited data in this example. Studies with more records should be performed in the future to have better perspectives.

4. Conclusion

A consistent spectral matching procedure of three-component seismic ground acceleration records was proposed. The procedure is straightforward, yet it is general. It preserves the couplings among the three components. It can be used with the phase record preserved, but also it serves when the phase difference is imposed between the modified and the seed records, or if a phase changed is desired. The former is especially beneficial when the periodic pattern of the records' phase needs to be maintained. The pattern was found in the five records considered in the example for all three components for up to 15 Hz frequency range and reported for the first time in this article. When the matching process is performed based on the Fourier spectral ratio, the solution is exact;

however, when the response spectral ratio is used then the solution is approximate, and an iteration scheme is necessary. In the latter, a target spectrum representing the three-component ground motion should be provided as the reference in the matching procedure. Good convergence in the velocity and displacement records was achieved, and no baseline correction was required.

Declarations

Funding: This research did not receive any specific grant from funding agencies in the public, commercial, or not-for-profit sectors.

Conflicts of interest/Competing interests: The authors acknowledge there are no conflicts of interest recorded.

Availability of data and material: Data employed in the study are taken from the sources listed in the references.

Code availability: No commercial software was used; all custom codes.

References

Abrahamson, N. A. (1992). Non-stationary spectral matching, *Seismol. Res. Lett.* **63**, no. 1, 30.

Adekristi, A. and Eatherton, M.R. (2016). Time-domain spectral matching of earthquake ground motions using Broyden updating, *J. Earthq. Eng.* **20**, no. 5, 679–698.

Al Atik, L. and Abrahamson, N.A. (2010). An improved method for non-stationary spectral matching, *Earthq. Spectra* **26**(3), 601–617.

ASCE/SEI (2005). Seismic Design Criteria for Structures, Systems, and Components in Nuclear Facilities, *ASCE/SEI Standard 43-05*. American Society of Civil Engineers.

Baker, J.W. and Lee, C. (2018). An Improved Algorithm for Selecting Ground Motions to Match a Conditional Spectrum, *J. Earthq. Eng.* **22**, no. 4, 708-723.

Bani-Hani, K.A. and Malkawi, A.I. (2017). A Multi-step approach to generate response-spectrum-compatible artificial earthquake accelerograms, *Soil Dynam Earthquake Eng*, **97**, 117-132.

Bazzurro, P. and N. Luco (2006). Do scaled and spectrum-matched near-source records produce biased nonlinear structural responses? *Proc. of the 100th Anniversary Earthquake Conf. Commemorating the 1906 San Francisco Earthquake*, San Francisco, California, 1–22 April, Paper Number 1029.

Bougioukou, A.P., Leros, L.P. and Papakonstantinou, V. (2008). Modeling of non-stationary ground motion using the mean reverting stochastic process, *Appl Math Model* **32**, 1912–1932.

Bozorgnia, Y. and Campbell, K.W. (2016). Ground Motion Model for the Vertical-to-Horizontal (V/H). Ratios of PGA, PGV, and Response Spectra, *Earthquake Spectra*, **32**(2), 951-978.

Carballo, J.E. and C.A. Cornell (2000). Probabilistic seismic demand analysis: Spectrum matching and design, Report No. RMS-41, Department of Civil and Environmental Engineering, *Reliability of Marine Structures Program*, Stanford University, Stanford, California.

Carlson, C., Zekkos, D. and Athanasopoulos-Zekkos, A. (2016). Predictive Equations to Quantify the Impact of Spectral Matching on Ground Motion Characteristics. Earthquake Spectra, *Earthq. Spectra* **32**(1), 125–142.

Fahjan, Y. and Ozdemir, Z. (2008). Scaling of Earthquake Accelerograms for Non-Linear Dynamic Analyses to Match the Earthquake Design Spectra, *Proc. of the Fourteenth World Conference on Earthquake Engineering*, Beijing, China.

Gao, Y., Wu, Y., Li, D., Zhang, N. and Zhang, F. (2014). An Improved Method for the Generating of Spectrum-Compatible Time Series Using Wavelets, *Earthq. Spectra* **30**(4), 1467–1485.

Gascot, R. L. and Montejo, L. A. (2016). Spectrum compatible earthquake records and its influence on the seismic response of reinforced concrete structures, *Earthq. Spectra* **32**(1), 101–123.

Gasparini, D. A. and Vanmarcke, E.H. (1976). SIMQKE: Simulated earthquake motions compatible with prescribed response spectra, Department of Civil Engineering, *Research Report R76-4*, Massachusetts Institute of Technology, Cambridge, Massachusetts, 65 pp

Ghaboussi, J. and Lin, C.J. (1998). New Method of Generating Spectrum Compatible Accelerograms Using Neural Networks, *Earthq. Eng. Struct. Dynam.* 36, no. 13, 1813–1835.

Ghaffarzadeh, H. and Izadi, M.M. (2008). Artificial Generation of Spatially Varying Seismic Ground Motion Using ANNs, *The 14th World Conference on Earthquake Engineering*, Beijing, China, 12-17 October.

Hancock, J., Watson-Lamprey, J., Abrahamson, N.A., Bommer, J.J., Markatis, A., McCoy, E. and Mendis, R. (2006). An improved method of matching response spectra of recorded earthquake ground motion using wavelets, *J. Earthq. Eng.* **10**, 67–89.

He, H., Li, R. and Chen, K. (2015). Characteristics of jerk response spectra for elastic and inelastic systems, *Shock Vib*, Article ID 782748.

Hong, L.L and Yu-Chiau Huang, Y.C (2020). A new algorithm in generating spectrum-compatible ground accelerograms, *J Chin Inst Eng*, **43**(3), 241-248.

Kaul, M. K. (1978). Spectrum-Consistent Time-History Generation, *J. Engineering Mechanics Division* (ASCE). **104** (4), 781–788.

Kohrangi, M., Bazzurro, P., Vamvatsikos, D. and Spillatura, A. (2017). Conditional spectrum-based ground motion record selection using average spectral acceleration, *Earthq. Eng. Struct. Dynam.* **46**, no. 10, 1667–1685.

Kost, G., Tellkamp, T., H. Kamil, H., Gantayat, A. and Weber, F. (1978). Automated generation of spectrum-compatible artificial time histories, *Nucl Eng Des* **45**(1), 243–249.

Lancieri, M., Bazzurro, P. and Scotti, O. (2018). Spectral Matching in Time Domain: A Seismological and Engineering Analysis, *Bull. Seismol. Soc. Am.* **108**, no. 4, 1972–1994.

Laurendeau, A., Cotton, F. and Bonilla, L.F. (2012). Nonstationary stochastic simulation of strong ground-motion time histories: Application to the Japanese database, *The 15th World Conf. on Earthquake Engineering*, Lisbon, Portugal, 24–28 September.

Lee, S.C. and Han, S.W. (2002). Neural-network-based models for generating artificial earthquakes and response spectra, *Comput Struct*, **80**(20-21), 1627-1638.

Li, B, Wei-Chau Xie, W.C and Pandey, M.D. (2016). Generate tri-directional spectra-compatible time histories using HHT method, *Nucl Eng Des* **308**, 73–85.

Lilhanand, K. and Tseng, W.S. (1988). Development and application of realistic earthquake time histories compatible with multiple damping response spectra, *Proc. of the Ninth World Conference on Earthquake Engineering*, Tokyo, Japan, Vol. 2, pp. 819–824.

Luco, N. and P. Bazzurro (2007). Does amplitude scaling of ground motion records result in biased nonlinear structural drift responses? *Earthq. Eng. Struct. Dynam.* **36**, no. 13, 1813–1835.

Mukherjee, S. and V. K. Gupta (2002). Wavelet-based characterization of design ground motions, *Earthq. Eng. Struct. Dynam.* **31**, no. 5, 1173–1190.

Naeim, F. and Lew, M. (1995). On the use of design spectrum compatible time histories, *Earthq. Spectra* **11**, 111-127.

Ni, S.H., Xie, W.C., and Pandey, M.D. (2011). Tri-directional spectrum-compatible earthquake time-histories for nuclear energy facilities, *Nucl Eng Des* **241**, 2732–2743.

Ohsaki, Y. (1979). On the Significance of Phase Content in Earthquake Ground Motions, *Earthq. Eng. Struct. Dynam.* **7**, 427–439.

Papadimitriou, K. (1990). Stochastic Characterization of Strong Ground Motion and Applications to Structural Response, *Report No. EERL 90-03, Earthquake Engineering Research Laboratory*, Pasadena, p. 12.

PEER (2020). Ground Motion Database, Pacific Earthquake Engineering Research Center. https://ngawest2.berkeley.edu/spectras/new?sourceDb_flag=1 (last accessed October 2020).

Pousse, G., Bonilla, L.F., Cotton, F. and L. Margerin (2006). Nonstationary stochastic simulation of strong ground motion time histories including natural variability: Application to the K-Net Japanese database, *Bull. Seismol. Soc. Am.* **96**, no. 6, 2103–2117.

Press, W.H., Teukolsky, S.A., Vetterling, W.T. and Flannery, B.P. (2007). *Numerical Recipes: The Art of Scientific Computing*, 3rd Ed., Cambridge University Press., 600-602.

Preumont, A. (1984). The generation of spectrum compatible accelerograms for the design of nuclear power plants, *Earthq. Eng. Struct. Dynam.* **12**, no. 4, 481–497.

Rizzo, P.C., Shaw, D.E., and Jarecki, S.J. (1975). Development of real/synthetic time histories to match smooth design spectra, *Nucl Eng Des* **32**, 148–155.

Roman-Velez, X. and Montejo, L.A. (2020). Generation of seed-based spectrum-compatible pulse-like time-series, *Bull Earthquake Eng* **18,** 1161–1186.

Seifried, A. E. and Baker, J.W. (2016). Spectral variability and its relationship to structural response estimated from scaled and spectrum matched ground motions, *Earthq. Spectra* **32**, no. 4, 2191–2205.

Shahbazian, A., and Pezeshk, S. (2010), Improved velocity and displacement time histories in frequency domain spectral-matching procedures, *Bull. Seismol. Soc. Am.* **100**, no. 6, 3213-3223.

Silva, W. J. and K. Lee (1987). WES RASCAL code for synthesizing earthquake ground motions, *Report 24. Misc. Paper S-73-1*, Department of the Army, US Army Corps of Engineers.

Suarez, L.E. and Montejo, L.A. (2005). Generation of artificial earthquake via the wavelet transform, *Int. J. Solids Struct.* **42**, 5905–5919.

Tao, D., Lin, J. and Lu, Z. (2019). Time-Frequency Energy Distribution of Ground Motion and Its Effect on the Dynamic Response of Nonlinear Structures, *Sustainability*, **11**(3), 702.

Thrainsson, H., Kiremidjian, A.S. and Winterstein, S.R. (2000). Modeling of Earthquake Ground Motion in the Frequency Domain, *Report No. 134, The John A. Blume Earthquake Engineering Centre*, Department Civil and Environmental Enginering, Stanford University, Stanford, California.

Tiliouine, B., M Hammoutene, M. and Bard, P.Y. (2000). Phase Angle Properties of Earthquake Strong Motions: A Critical Look, *Proc. of the Twelfth World Conference on Earthquake Engineering*, Auckland, New Zealand.

Waezi, Z. and Rofooei, F.R. (2017). Stochastic Non-Stationary Model for Ground Motion Simulation Based on Higher-Order Crossing of Linear Time Variant Systems, *J. Earthq. Eng.* **21**, 123–150.

Wang, G., Youngs, R., Power, M. and Li, Z. (2014). Design ground motion library (DGML): an interactive tool for selecting earthquake ground motions, *Earthq. Spectra* **31**, 617–635.

Zekkos, D., Carlson, C., Nisar, A. and Ebert, S. (2012). Effect of ground motion modification technique on seismic geotechnical analyses, *Earthq. Spectra* **28**(4), 1643-1661.

Zentner, I. (2013). Simulation of non-stationary conditional ground motion fields in the time domain, *Georisk Assess. Manag. Risk Eng. Syst. Geohazards,* **7**, no. 1, 37–48.

Appendix

The general form of the stationary spectral ratio filter function can be expressed as follows,

$$P(\omega) = |P(\omega)|\, e^{i\phi_P(\omega)} = P_R(\omega) + i\, P_I(\omega) \tag{A1}$$

where the real and imaginary parts are $P_R(\omega) = |P(\omega)|\, cos\, \phi_P(\omega)$ and $P_I(\omega) = |P(\omega)|\, sin\, \phi_P(\omega)$, respectively. Let's suppose that the real part takes the form of

$$P_R(\omega) = \alpha(\omega)\, S_R(\omega) \tag{A2}$$

where $\alpha(\omega)$ is a non-negative frequency dependent function to be determined and $S_R(\omega)$ is a spectral ratio defined as the ratio of the target spectrum with respect to that of the record of interest, or $S_R(\omega) = FAS_{\mathbf{u}t}(\omega) / FAS_{\mathbf{u}}(\omega)$ or $S_R(\omega) = S_{\mathbf{v}t}(\omega) / S_{\mathbf{v}}(\omega)$, for the Fourier or response spectra, respectively. With Eq. (A2), Eq. (A1) becomes,

$$P(\omega) = \frac{\alpha(\omega)\, S_R(\omega)}{cos\, \phi_P(\omega)} \left[cos\, \phi_P(\omega) + i\, sin\, \phi_P(\omega) \right] \tag{A3}$$

where $|P(\omega)| = \dfrac{\alpha(\omega)\, S_R(\omega)}{cos\, \phi_P(\omega)}$. Now, let us suppose that $|P(\omega)| = S_R{}^{\beta}(\omega)$ for $0 \le \beta \le 1$; then it follows,

$$0 \le cos\, \phi_P(\omega) = \alpha(\omega)\, S_R{}^{1-\beta}(\omega) \le 1. \tag{A4}$$

Substitute Eq. (A4) into Eq. (A3) to obtain the following,

$$P(\omega) = S_R{}^{\beta}(\omega)\, e^{i\phi_P(\omega)} \tag{A5}$$

and $$tan\,\phi_P(\omega)=\sqrt{\left(\frac{S_R{}^{\beta-1}(\omega)}{\alpha(\omega)}\right)^2-1} \tag{A6}$$

where $$\alpha(\omega)\le S_R{}^{\beta-1}(\omega). \tag{A7}$$

Eq. (A5) is the general form of the spectral ratio filter function for any $0\le\beta\le1$. The following two cases deserve more remarks.

Case 1: $\phi_P(\omega)=\theta(\omega)$ is a given phase difference (including constant or zero). For β=0, Eq. (A5) involves no spectral matching; for β=1 the operation is an amplitude varying spectral matching.

Case 2: $\phi_P(\omega)$ is a variable. If $\alpha(\omega)=S_R{}^{\beta-1}(\omega)$ (see Eq. (A7)) the filter phase is identically zero (from Eq. (A6)). If, further, β=0 the operation involves no record change; if β=1 the operation is a zero-phase spectral matching. If $\alpha=S_R{}^{\beta-1}(\omega)\big|_{min}$, constant, then $0\le\phi_P(\omega)\le\pi/2$. If, further, β=0 the operation is a unit amplitude spectral matching; if β=1 it is a zero-phase spectral matching.

List of Figures:

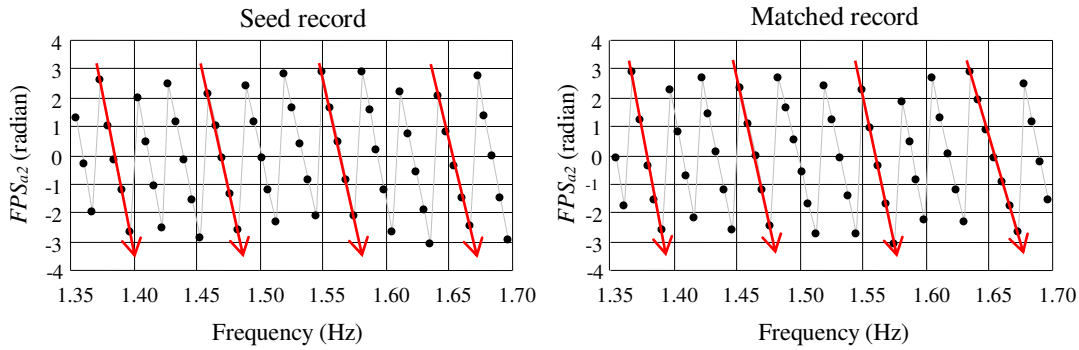

Figure 1 The Fourier phase spectrum [-π,π] of the seed and that of the matched records (component 2). The dots are the FFT sampling points; they form certain periodic pattern shown by the red arrow pointing in the increasing frequencies. The pattern exists for frequency range up to 15 Hz, all three components, and all five earthquakes in Table 1.

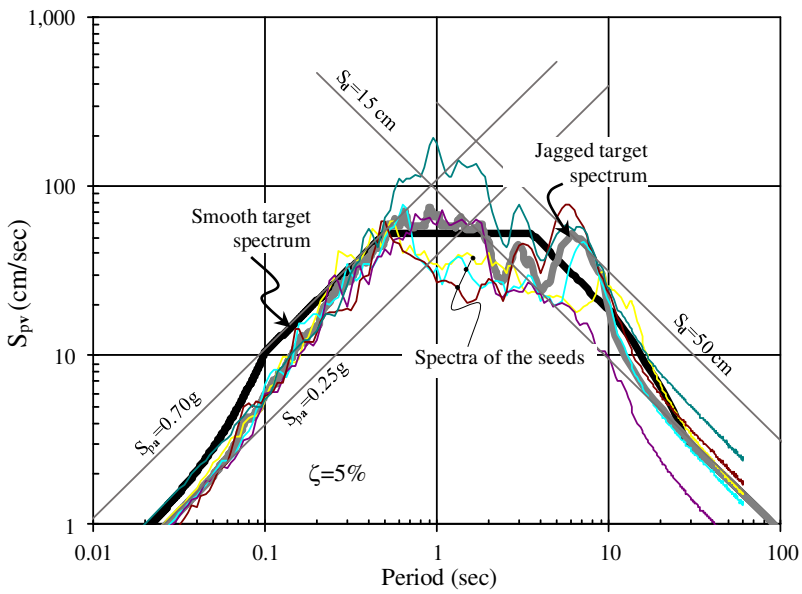

Figure 2 The smooth, the five seed records, and the jagged spectra as the average of those five. The smooth spectrum was generated by the SRSS combination of the vertical and horizontal spectra; while the seed spectra were derived based on Eq. (2), 5% damping. Smooth spectra: PGA= 0.3g, PGD=14.3 cm. Jagged spectra: PGA= 0.24g, PGD=14.3 cm.

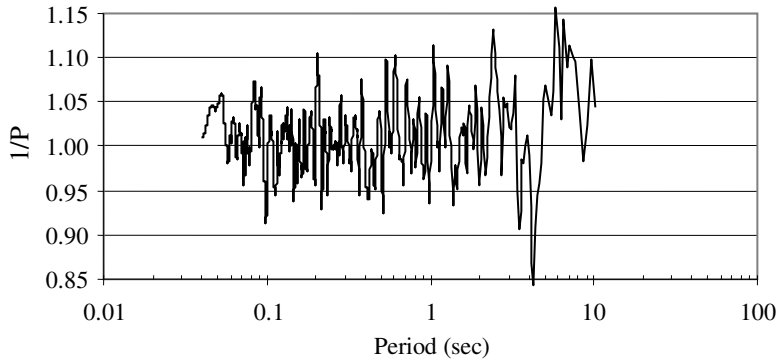

Figure 3 The reciprocal of the spectral ratio of the matched record to that of the target, $1/P(T)$; its average is 1.007.

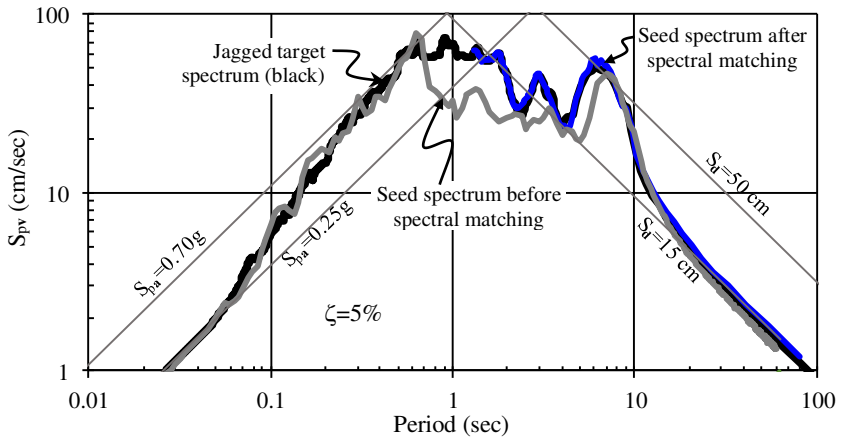

Figure 4 The jagged target spectrum for spectral matching of Chuetsu-oki record whose pre- and post-spectral matching pseudo velocity spectra are shown (ζ=5%). The target PGA=0.24g and PGD=14.3 cm.

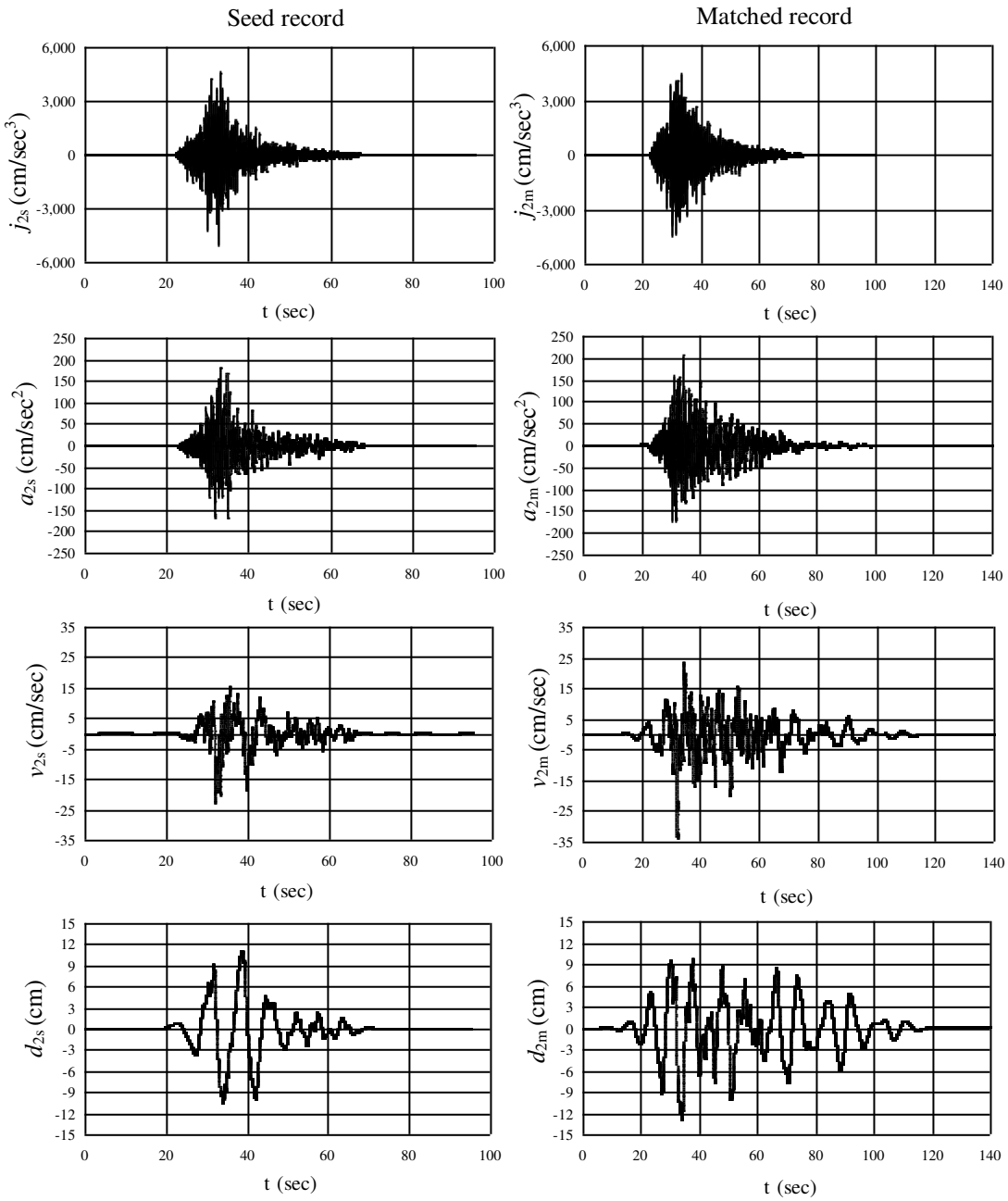

Figure 5 The major component of the jerk, acceleration, velocity, and the displacement of the seed (left) and matched (right) records against the jagged spectra. Their only difference was only in their respective Fourier amplitude spectra.

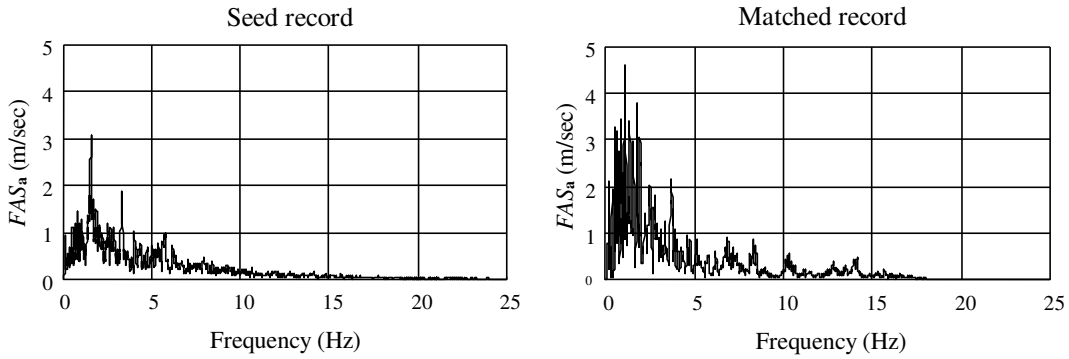

Figure 6 The acceleration Fourier amplitude spectra of the seed and the matched records against the jagged target spectra. $FAS_{\mathbf{a}}(\omega)=\sqrt{\mathbf{A_a}(\omega)\bullet\mathbf{A_a}^*(\omega)}$ where $\mathbf{A_a}^*(\omega)$ is the conjugate of $\mathbf{A_a}(\omega)$, the symbol $\bullet$ is for inner product.

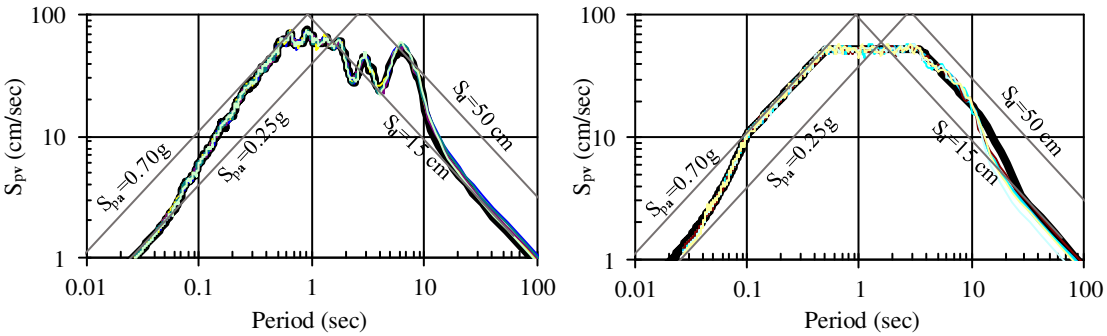

Figure 7 The pseudo velocity spectra after the spectral matching against the jagged (left) and the smooth (right) spectra. All converge to the target at period up to 10 seconds.

List of Tables:

Table 1 Seismic seed records employed in the example of the section

Event	Origin	Date	Station	PGA (g)	M_w	R_{jb} (km)
Chi-Chi	Taiwan	1999	CHY010	0.25	7.6	20
Chuetsu-oki	Japan	2007	Matsushiro Tokamachi	0.23	6.8	18
Darfield	New Zealand	2010	SPFS	0.22	7.0	30
Iwate	Japan	2008	Semine Kurihara City	0.19	6.9	29
Chi-Chi	Taiwan	1999	CHY034	0.33	7.6	15

M_w: moment magnitude; PGA: peak ground acceleration; R_{jb}: Joyner-Boore distance

Table 2 Some ground motion parameters of the Chuetsu-oki record before and after modification against the jagged target spectrum

	Target	Seed	Matched
PGA (g)	0.24	0.23	0.24
PGV (m/s)	-	0.236	0.370
PGD (m)	0.143	0.125	0.145
I_A (m/s)	-	1.34	2.93
$D_{05\text{-}95}$ (s)	-	19.48	29.20

PGA,PGV,PGD: peak ground acceleration, velocity, and displacement, respectively

I_A: Arias intensity; $D_{05\text{-}95}$: significant duration

Table 3 Some ground motion parameters and their variations

			The average of the five records			The coefficient of variations		
	Target		Seed	Matched		Seed	Matched	
	Smooth	Jagged		Smooth	Jagged		Smooth	Jagged
PGA (g)	0.30	0.24	0.24	0.28	0.24	0.21	0.05	0.02
PGV (m/s)	-	-	0.29	0.25	0.31	0.45	0.16	0.15
PGD (m)	0.143	0.143	0.146	0.124	0.149	0.42	0.12	0.05
I_A (m/s)	-	-	2.05	3.48	3.01	0.45	0.16	0.09
$D_{05\text{-}95}$ (s)	-	-	22.90	28.19	31.77	0.18	0.20	0.14

PGA,PGV,PGD: peak ground acceleration, velocity, and displacement, respectively

I_A: Arias intensity; $D_{05\text{-}95}$: significant duration